

The ZIMPOL high contrast imaging polarimeter for SPHERE: sub-system test results

Ronald Roelfsema^a, Daniel Gisler^b, Johan Pragt^a, Hans Martin Schmid^b, Andreas Bazzon^b, Carsten Dominik^j, Andrea Baruffolo^c, Jean-Luc Beuzit^d, Julien Charton^d, Kjetil Dohlen^e, Mark Downing^f, Eddy Elswijk^a, Markus Feldt^h, Menno de Haan^a, Norbert Hubin^f, Markus Kasper^f, Christoph Kellerⁱ, Jean-Louis Lizon^f, David Mouillet^d, Alexey Pavlov^h, Pascal Puget^d, Sylvain Rochat^d, Bernardo Salasnich^c, Peter Steiner^b, Christian Thalmann^j, Rens Watersⁱ, Francois Wildi^k

^aNOVA-ASTRON, Oude Hoogeveensedijk 4, 7991 PD Dwingeloo, The Netherlands;

^bInstitute of Astronomy, ETH Zurich, 8093 Zurich, Switzerland;

^cINAF, Osservatorio Astronomico di Padova, 35122 Padova, Italy;

^dIPAG, Université Joseph Fourier, BP 53, 38041 Grenoble cedex 9, France;

^eLESIA, Observatoire de Paris, 5 place J. Janssen, 92195 Meudon, France;

^fESO, Karl-Schwarzschild-Strasse 2, D-85748 Garching bei München, Germany

^gLAM, UMR6110, CNRS/Universite de Provence, 13388 Marseille cedex 13, France;

^hMax-Planck-Institut für Astronomie, Königstuhl 17, 69117 Heidelberg, Germany;

ⁱSterrekundig Instituut Utrecht, Princetonplein 5, 3584 CC Utrecht, The Netherlands;

^jAstronomical Institute “Anton Pannekoek”, 1098 SJ Amsterdam, The Netherlands;

^kObservatoire Astronomique de l’Université de Genève, 1290 Sauverny, Switzerland

ABSTRACT

SPHERE (Spectro-Polarimetric High Contrast Exoplanet Research) is one of the first instruments which aim for the direct detection from extra-solar planets. The instrument will search for direct light from old planets with orbital periods of several months to several years as we know them from our solar system. These are planets which are in or close to the habitable zone. ZIMPOL (Zurich Imaging Polarimeter) is the high contrast imaging polarimeter subsystem of the ESO SPHERE instrument. ZIMPOL is dedicated to detect the very faint reflected and hence polarized visible light from extrasolar planets. The search for reflected light from extra-solar planets is very demanding because the signal decreases rapidly with the orbital separation. For a Jupiter-sized object and a separation of 1 AU the planet/star contrast to be achieved is on the order of 10^{-8} for a successful detection. This is much more demanding than the direct imaging of young self-luminous planets. ZIMPOL is located behind an extreme AO system (SAXO) and a stellar coronagraph. SPHERE is foreseen to have first light at the VLT at the end of 2012. ZIMPOL is currently in the subsystem testing phase. We describe the results of verification and performance testing done at the NOVA-ASTRON lab. We will give an overview of the system noise performance, the polarimetric accuracy and the high contrast testing. For the high contrast testing we will describe the impact of crucial system parameters on the contrast performance. SPHERE is an instrument designed and built by a consortium consisting of IPAG, MPIA, LAM, LESIA, Fizeau, INAF, Observatoire de Genève, ETH, NOVA, ONERA and ASTRON in collaboration with ESO.

Keywords: Extra-solar planets, imaging, polarimetry, high-contrast

1. INTRODUCTION

1.1 ZIMPOL science case

SPHERE-ZIMPOL^{1,2,3,4} (Spectro-Polarimetric High Contrast Exoplanet Research - Zurich Imaging Polarimeter) is one of the first instruments which aim for the direct detection of reflected light from extra-solar planets. The instrument will search for direct light from old planets with orbital periods of a few months to a few years as we know them from our solar system. These are planets which are in or close to the habitable zone.

The reflected radiation is generally polarized and the degree of polarization may be particularly high at short wavelengths $< 1\mu\text{m}$ due to Rayleigh scattering by molecules and scattering by haze particles in planetary atmospheres^{5,6}. For this reason the visual-red spectral region is well suited for planet polarimetry.

The search for reflected light from extra-solar planets is very demanding, because the signal decreases rapidly ($\sim 1/a^2$) with the orbital separation a . For a Jupiter-sized object and a separation of 1 AU the planet/star contrast to be achieved is on the order of 10^{-8} for a successful detection. This is much more demanding than the direct imaging of young self-luminous planets.

Therefore SPHERE-ZIMPOL will be capable to investigate only the very nearest stars for the polarization signal from extra-solar planets. There are half a dozen of good candidate systems for which giant planets should be detectable, even if their properties are not ideal (low albedo, not highly polarized). In another handful targets there is some chance to find high-polarization planets, if they exist around them. For stars further away a detection of reflected light with SPHERE-ZIMPOL will be difficult.

Besides the search for extra-solar planets the ZIMPOL high precision imaging polarimetry will certainly be very powerful for the investigation of the scattering polarization from circumstellar disks and dust shells around bright young and evolved stars. ZIMPOL can also be used in non-polarimetric mode for coronagraphic and non-coronagraphic high contrast imaging in the 550 – 900 nm range for the investigation of the circumstellar regions around stars bright enough for wave front sensing (about $R < 10$ mag). The system will provide a diffraction limited resolution of 16 mas in the R-band with an AO Strehl ratio of up to 50%.

1.2 SPHERE-ZIMPOL outline

ZIMPOL is one of the four sub-systems of SPHERE⁷ (figure 1). The design of SPHERE is divided into four subsystems: the Common Path and Infrastructure (CPI) and the three science channels: a differential imaging camera (IRDIS⁸, Infrared Dual Imager and Spectrograph), an Integral Field Spectrograph (IFS), and a visible imaging polarimeter (ZIMPOL). Refer to previous articles for detailed design and performance description

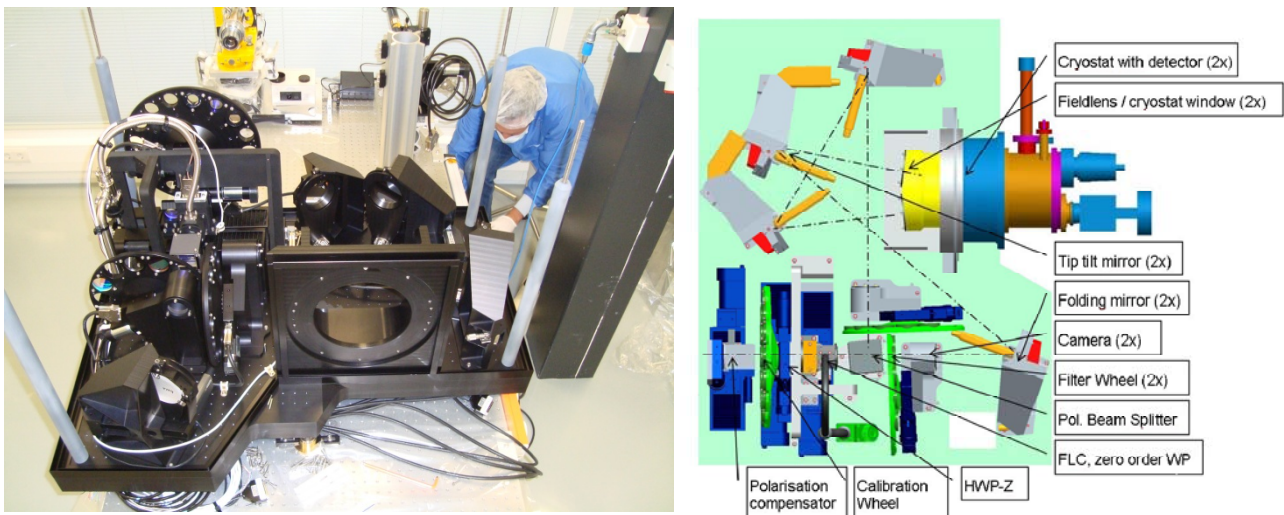


Figure 1. (Left) The ZIMPOL bench during integration. (Right) Components on the ZIMPOL bench.

Among ZIMPOL's main specifications are a bandwidth of 600 to 900 nm (with a goal of 500 to 900 nm) and an instantaneous field of view of 3×3 arcsec² with access to a total field of view of 8 arcsec diameter by an internal field selection mechanism. The ZIMPOL optical train contains a common optical path that is split with the aid of a polarizing beamsplitter in two optical arms. Each arm has its own detector. The common path contains common components for both arms like calibration components, common filters, a switchable half wave plate and a Ferro Electric Liquid (FLC) crystal polarization modulator. The two arms have the ability to measure simultaneously the two complementary polarization states in the same or in distinct filters. The images on both ZIMPOL detectors are Nyquist sampled at 600 nm. The detectors are both located in the same cryostat and cooled to -80 °C. The rest of the ZIMPOL opto-mechanical system is at ambient temperature.

Because the degree of polarization of a planet is measured relative to the local background light (from the central star) it can in principle be obtained with very high accuracy without the need for an absolute instrument calibration.

ZIMPOL can be used in three polarimetric modes as well as in a classical imaging mode.

1.3 ZIMPOL specifications

ZIMPOL shall provide a high sensitivity linear polarization measurement for a localized signal near a bright source thanks to the simultaneous imaging of opposite polarization states (e.g. I_0 and I_{90}) with a fast polarimetric modulation – demodulation technique.

This observation mode shall make possible to achieve a contrast of 10^{-8} in 4 hr (goal 3×10^{-9} in 15 hr) for a 30% polarized planet at 1'' from a $I = 2.5$ mag star with SNR = 5.

Spectral range	600 – 900 nm (goal 500 – 900 nm)
Field of View (instantaneous)	3×3 arcsec ²
Field of View (total)	8 arcsec diameter
Wave Front Error	< 75 nm (goal < 50 nm)
Transmission	> 0.25 (goal > 0.40)
Polarimetric Sensitivity	< 10^{-5}
Polarimetric Accuracy	< 10^{-3}
Polarimetric Efficiency	> 0.75

2. ZIMPOL SUB-SYSTEM TEST RESULTS

2.1 Wave Front Error

The image quality of the ZIMPOL subsystem has been estimated based on the measurement reports of the individual optical components. The ZIMPOL RMS WFE is estimated as 45 nm and therefore it can be concluded that ZIMPOL is within the 50 nm RMS goal specification.

2.2 Transmission

The overall ZIMPOL transmission has been estimated based on the measurement reports of the individual optical components. The results of the individual components as well as the overall transmission can be found in Figure 2. The average transmission over the 600-900 nm band amounts to 0.51. It can be concluded that ZIMPOL is within 0.40 transmission goal specification.

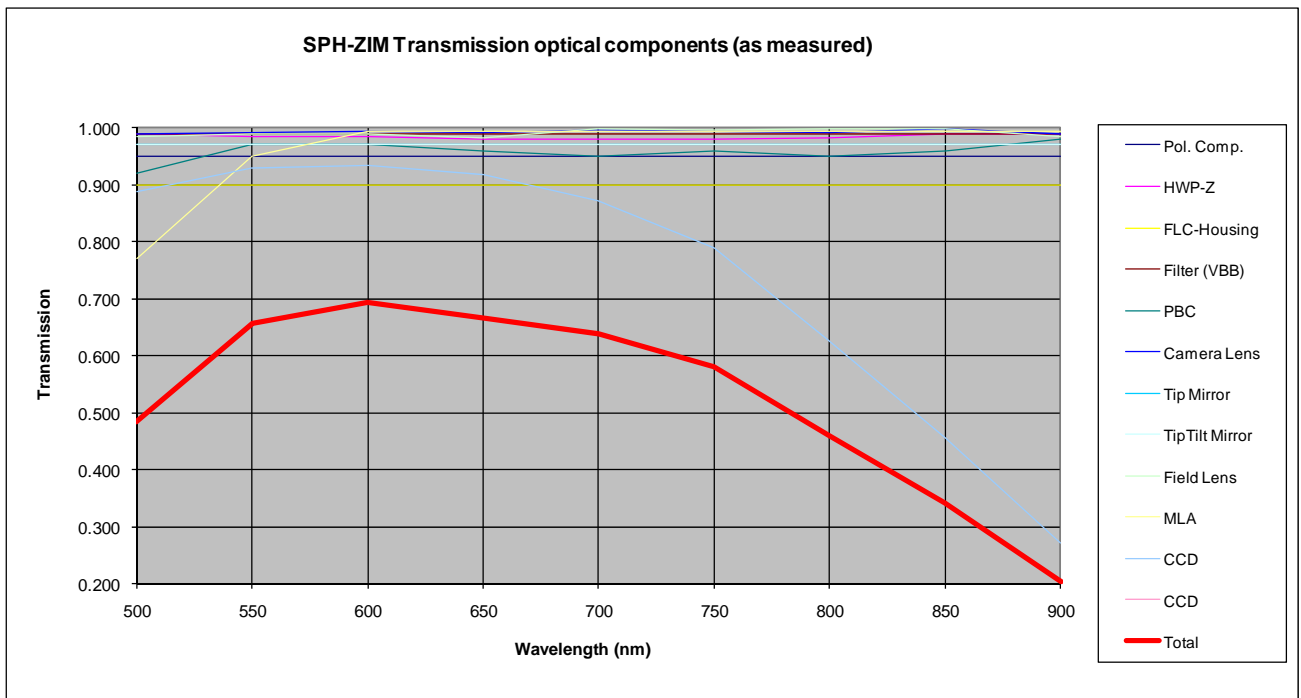


Figure 2 Transmission of the ZIMPOL components.

2.3 PSF Quality

The PSF quality and the Strehl ratio for ZIMPOL have been verified in various broad-band and narrow band filters. Figure 3 shows an example for the I-long filter at 870 nm.

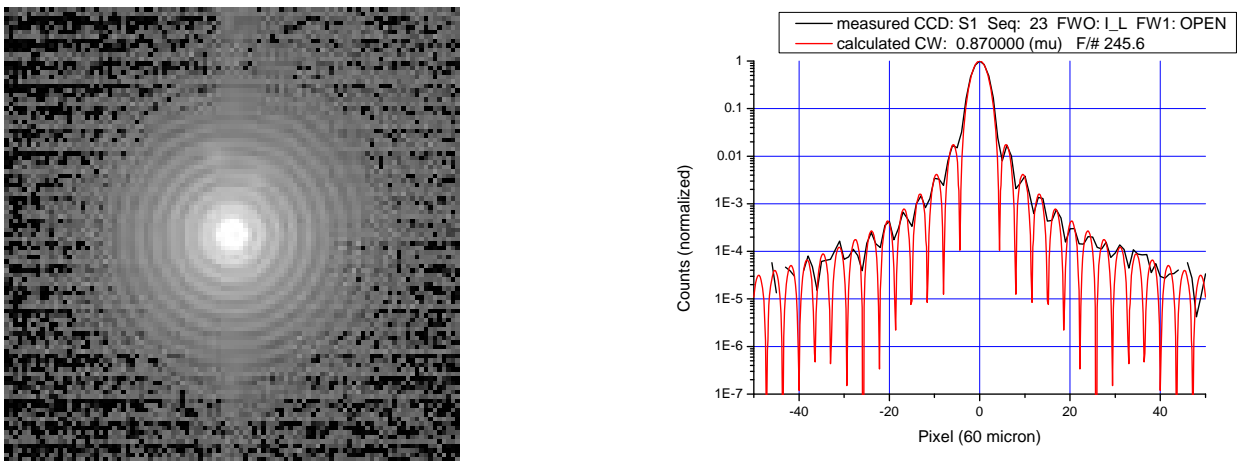


Figure 3 (Left) Image of the PSF for the I-Long Filter at 870 nm. (Right) A horizontal trace of the left image overlaid with the theoretical diffraction pattern.

For the pre-optics used in the test setup we have measured a WFE of about $\lambda/20$ (633 nm). For ZIMPOL we have calculated a WFE of about $\lambda/17$ (633 nm) (excluding any filters) and for a filter we assume a WFE of $\lambda/20$ (633 nm). These numbers result in a RMS WFE of 58 nm at 633 nm. In Figure 4 we have plotted the measured Strehl values and

calculated Strehl values based on the numbers given above. In general we see a reasonable correspondence between measurements and theory. From the plot we can conclude that apparently the RMS WFE is slightly better than expected.

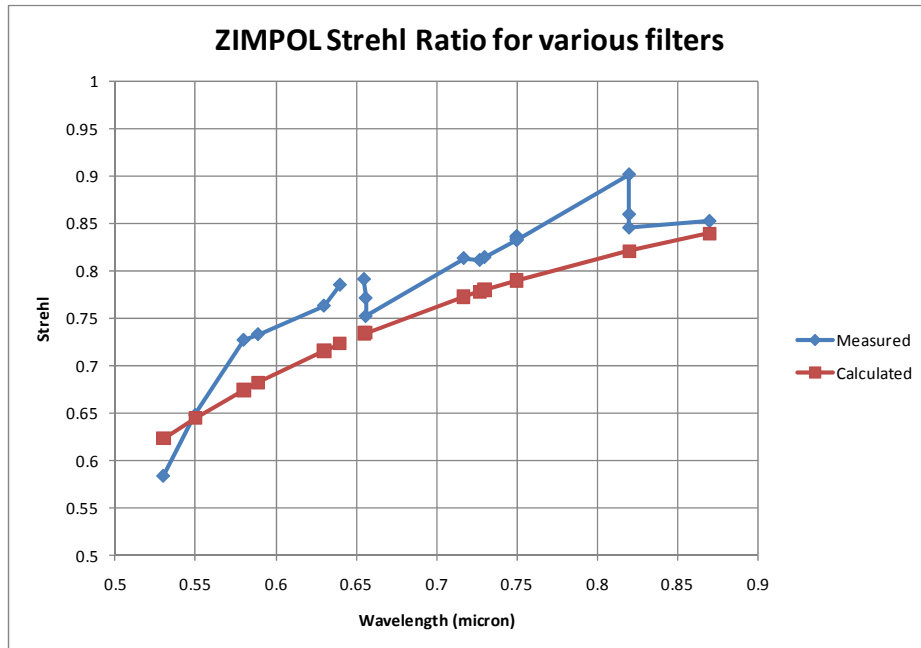


Figure 4 ZIMPOL measured and calculated Strehl Ratio for all filters.

2.4 Detector System

ZIMPOL uses two e2v frame transfer CCD44-82 2K x 4K Standard Silicon CCDs, one for each of the two polarization arms. The CCD's are located in an ESO modified Double e2v Detector Head and Continuous Flow Cryostat (see Figure 5). The detectors are controlled by NGC.

The ZIMPOL detectors 1 and 2 are very clean and have only of the order ~20 low (~50% or less) efficiency pixels / pixel pairs. There are another ~20 with less reduced efficiency (~60-80%). There are some extended features with reduced count rates on flat field exposures which can most likely be associated with "dirt" or other surface errors on the detectors, the micro-lens / stripe mask system or perhaps the field lens. However, the number of these features is very low.

The CCDs perform in ZIMPOL the polarimetric demodulation of the signal. Therefore, every second binned pixel row of the CCD is masked so that photon-charges created in the unmasked row during one half of the modulation cycle can be shifted for the second half of the cycle to the next masked row, which is used as temporary buffer storage. In this way the images for the two opposite polarization modes are registered with one pixel but then separated in two pixels in the detector image plane. The CCDs perform during the integration and demodulation in the image area also the read-out of the previous image in the read-out area. It is obvious that the operation of the CCDs in ZIMPOL is quite special and the thorough testing of the performance of these detector modes is essential.

Bias stability

Extensive bias stability measurements were made. For example, we measured the count level of the the overscan regions in fast polarimetry for 200'000 frames taken during 90 hours. For this time series the bias level showed the following excellent bias properties:

- Maximum excursions: 6 counts (max. to min.) for CCD1, 3 counts for CCD2
- Long term trend over 90 hours: less than 3 counts
- Typical frame to frame noise: +/- 1 count

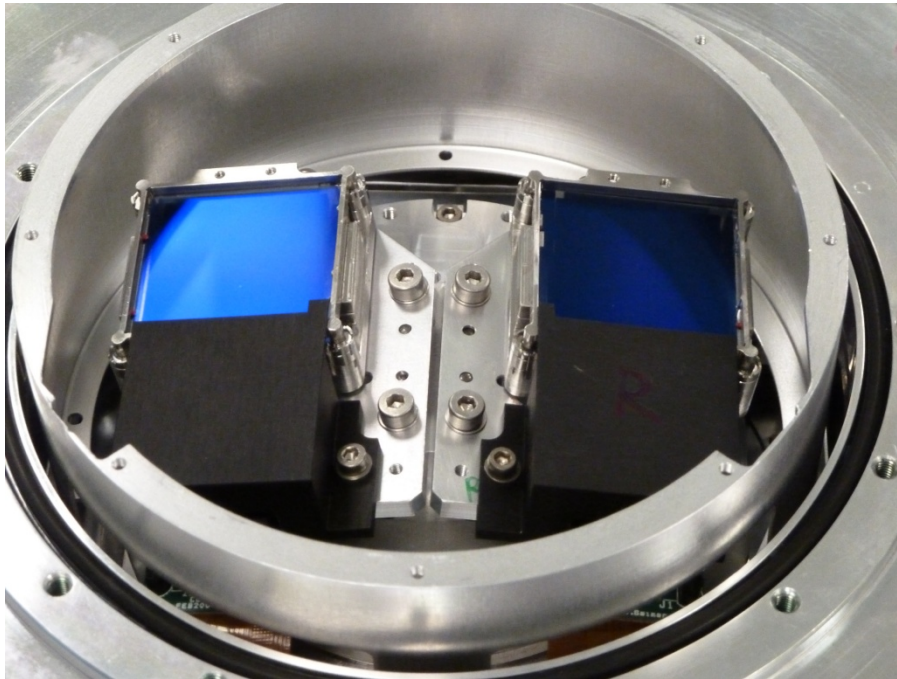


Figure 5 The two ZIMPOL CCDs S1 (left) and S2 (right) mounted and aligned in the cryostat. The read-out area is shielded with a black cover.

The different effects do not multiply like efficiency products. For example the temporal effect of the charge up and down shifting (demodulation) becomes only critical if the temporal modulation efficiency of the FLC modulator is significantly higher. Measurements of the overall modulation / demodulation efficiency of ZIMPOL were carried out:

- The obtained value in slow polarimetry mode was 90% for ZIMPOL arm 1 and 86% for arm 2.
- For fast polarimetry the measured efficiency was 82% for arm 1 and 77% for arm 2.

These values are within the specification of 75% but miss in fast polarimetry the goal of 90% quite a bit. It is certainly worth to consider how to improve a few percent on this.

We have assessed carefully the demodulation efficiency of the ZIMPOL detector. The demodulation efficiency is reduced by charge leaking and photon diffusion into the wrong rows mainly during integration / de-modulation and during frame transfer.

The charge and photon leakage or the row-to-row cross talks were measured for different colors in imaging mode (without charge shifting). The cross talk is quantified as charges in the covered pixels relative to the charges in the illuminated open pixel rows. Detailed measurements yield a value of around 3% - 4% (counts in covered rows / counts in open rows). The values depend slightly on wavelength with the best performance of 2.8%-3.7% in the R and I band. This effect depends also on the pixel position on the CCD because the micro-lens and stripe mask is well but not perfectly aligned with the pixel rows. The measured field depend effects in the demodulation efficiency is at a level of 4% or less.

During frame transfer light of the wrong polarization falls onto the image-rows. The effect is stronger for shorter integrations and it depends on the presence of a bright source in a given column. For flat field illumination the measured effect is at a level of 0.5 % for a 5s integration (in full frame mode). The expected effect is about 2% for a 1.2s integration and <0.1% for integrations longer than 20s.

It is important for efficient observations with the ZIMPOL polarimeter that the dependencies of the polarimetric efficiency on the different detector modes are well understood. Up to 10% of the observing time can easily be wasted by not choosing the wrong detector mode for polarimetry. Also the field dependent effects must be studied in more detail in order to assess the possible need and importance of field dependent polarimetric calibrations and corrections.

2.5 Modulator

In SPHERE-ZIMPOL the modulator is a switchable half wave plate based on a Ferroelectric Liquid Crystal (FLC) element working at a frequency of about 1 kHz.

Bumpy background

Figure 6 shows the polarization image (with a cross section on the right side) of a typical flat field measurement. The background shows variations in polarization of about 10^{-4} with a period of about 50 pixels. This so call “bumpy background” was an unexpected effect caused by the FLC modulator. Four of our five FLC modulators are affected by this effect.

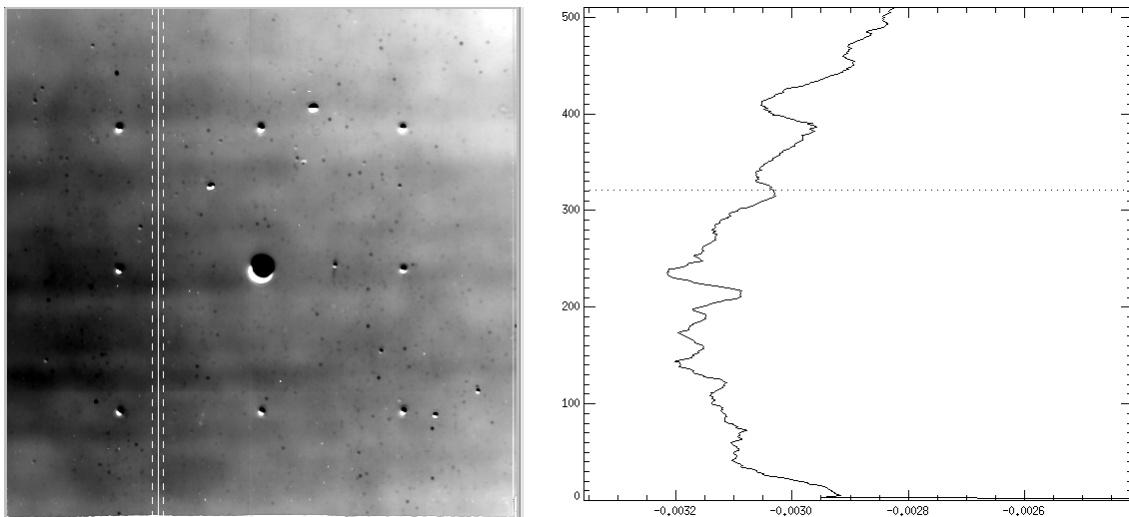


Figure 6 (Left) Polarization image that clearly shows a wavy horizontal pattern that is referred to as ‘Bumpy Background’ (Right) Vertical trace of the line as indicated in the left image.

These FLC modulators show a fine line pattern in the clear aperture (see Figure 7). We have discussed the effect with the manufacturer. He calls these line pattern zig-zag defects and they typically occur due to some sort of stress on the FLC modulator (e.g. changes in temperature or pressure). This defect is basically a change in the default orientation of the liquid crystal. It happens because there are two default orientations which the liquid crystal can take. In many instances these defects can be removed by a thermal cycling procedure. We have performed this procedure on one of the spare FLC modulators at ETH Zurich. These tests indicates that thermal cycling could improve the quality of the affected devices but since we have not yet installed and tested this particular modulator in SPHERE-ZIMPOL it is not possible to say if a thermal cycled device still shows a “bumpy background”.

Beam Shift

In Figure 6 there are also several asymmetric (black and white) polarization features. The features are artificial polarization signals which are caused by a small beam shift between the two FLC modulator states in combination of an intensity gradient. From the amplitude of the asymmetric signal one can calculate the shift of the beam on the detector.

For the currently installed FLC modulator we found a value of about $1.4\mu\text{m}$. compared with other measurement from previous tests this value is rather large.

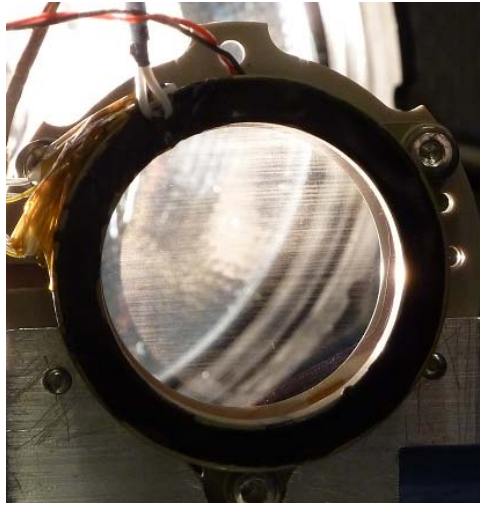


Figure 7 Fine (horizontal) line pattern that shows up in the FLC clear aperture

2.6 Noise Performance

The ZIMPOL noise performance has been measured by taking long duration flat fields and with a half-wave plate (HWP2) located close to the light source. For each run 20000 frames with HWP2 at 0 degree and 20000 frames with HWP2 at 45 degree were recorded. For all tests a broadband filter (bandwidth 290nm, center wavelength 740nm) has been used.

In the coronagraphic focus a coronagraphic mask with an additional astrometrical dot grid was installed. The substrate of the mask was rather dirty and with some scratches and digs on it. The goal to use this mask was to determine the limitation of the noise performance for polarimetry of strong intensity gradients, dust particles and small defects.

To calculate the polarization images only the basic ZIMPOL data reduction steps have been performed (bias subtraction and calculation of the polarization signal). No further calibrations (e.g. flat field correction and polarimetric efficiency calibration) have been achieved. The single polarization images were combined in two different modes:

Single difference	Images of one series in one HWP2 orientation has been averaged.
Double difference	Images of both series (HWP2 in 0 and 45 degree position) has been averaged.

Polarization images

Figure 8 shows the average of all polarization images of the measurement with a very low incoming polarization offset ($>0.01\%$). In the image of the measurement in single difference one can see the following effects:

- Many mostly horizontal background variations at the level of 10^{-4} which are the “bumpy background” problem of the FLC modulator described in the previous section
- Large scale variations of the background (gradients) at the level of a few 10^{-4} .
- For each dot and large dirt features on the astrometrical mask a strong asymmetric artificial signals caused by the FLC beam shift effect (also described in previous section)
- Many small signals (dots) which are most likely “real” polarization signals caused by small dust particles or scratch and digs on the substrate of the coronagraphic mask.

All these effects limit the noise performance in single difference measurements.

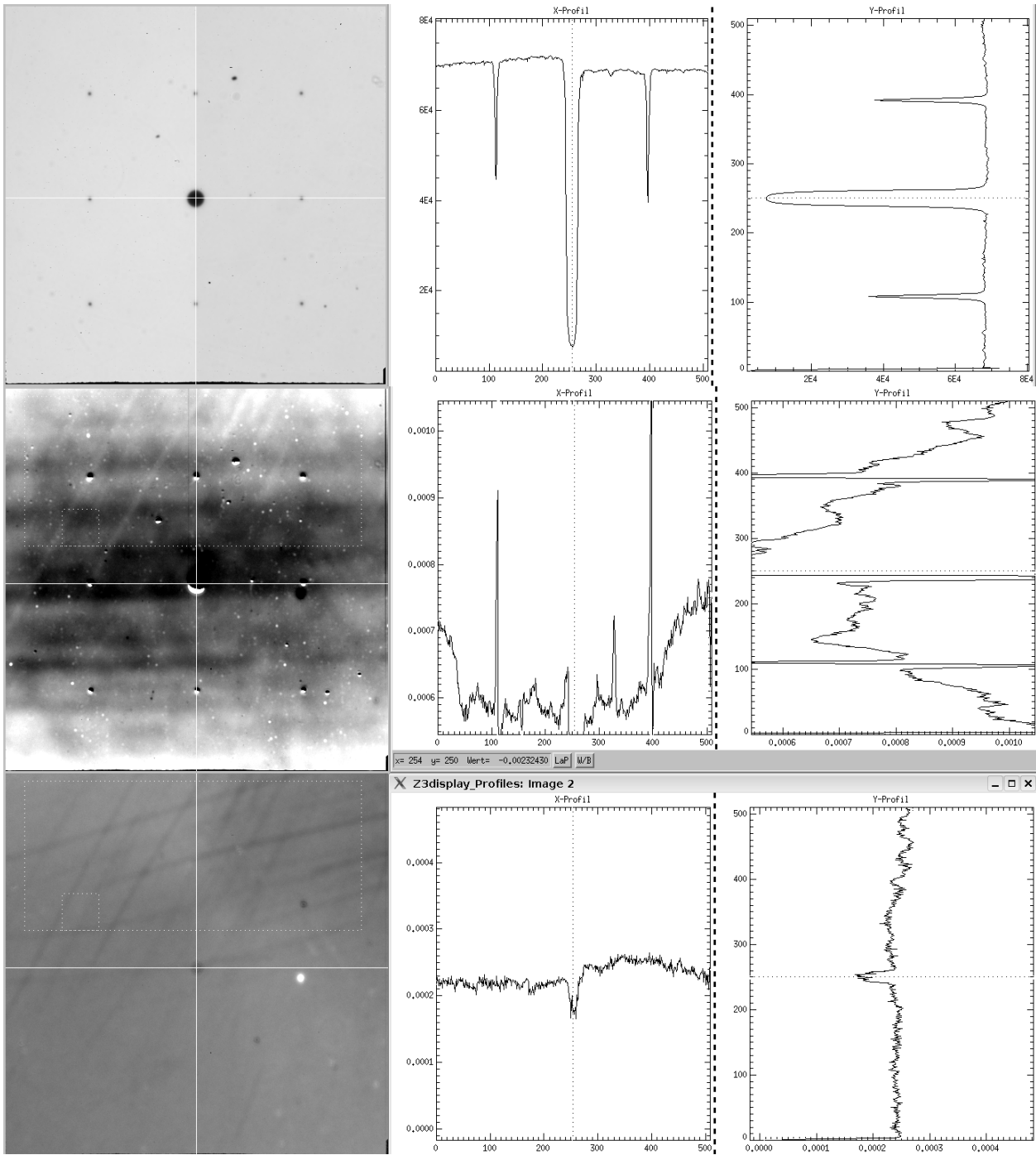


Figure 8 Average of all polarization images of the measurement with a very low incoming polarization offset ($> 0.01\%$).
 (Top) Intensity image (Middle) Single Difference image (Bottom) Double Difference image.

If one applies double difference technique most of the effects seen in single difference are removed to a very low level but a few effects are still visible:

- A signal of about $5 \cdot 10^{-5}$ in the coronagraphic mask

- Lines structures with polarization amplitude of a few 10^{-5} . These lines are caused by scratches on the HWP2 aperture. The scratches appear twice in the polarization image (for 0 and 45 degree position of HWP2).
- A few polarized dot structures (one with $5 \cdot 10^{-4}$, two with about 10^{-4} , and several with about 10^{-5} in polarization). These dots are most likely also caused by defects on HWP2.

This example measurement shows that in double difference the limiting factor for the noise performance is the optical quality of HWP2. In the test setup HWP2 was located very close to a focal plane. In the final instrument configuration HWP2 will be located father away from a focal plane and therefore one can expect these features will be strongly reduced.

Noise performance

To quantify the noise the standard deviation was calculated on a small (50x50 pixel) part of the polarization images and compared to the theoretical limiting noise level calculated from the numbers of detected photons.

A high background polarization often has a negative impact on the small scale noise performance of a ZIMPOL type polarimetry. Therefore the noise performance tests have been done with different incoming background polarization.

Figure 9 shows the measured small scale noise level as function of detected photons for four different background polarizations and the measurement without modulator. The measurement without modulator shows that the detector system is photon noise limited already in single difference down to at least $4 \cdot 10^{-6}$. A background polarization up to 1% has no significant impact on small scale noise in single and double difference.

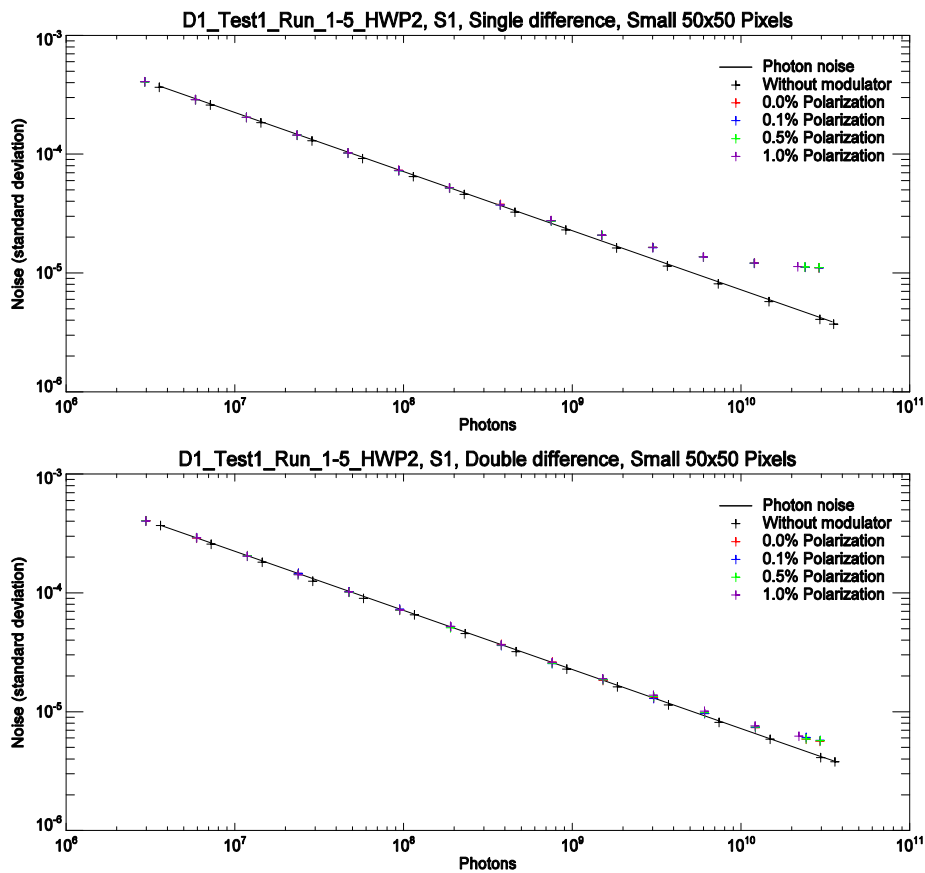


Figure 9 Noise as function of number of photons for various levels of background polarization. The straight line indicates the photon noise limit. (Top) Single Difference (Bottom) Double Difference.

2.7 High Contrast Imaging

Simulating the detection of an exoplanet in the lab requires a small polarized signal close to an unpolarized bright point source. For this purpose a fiber based star-planet simulator has been build. For high contrast measurements the intensity of the planets is reduced by ND filters and the star flux is attenuated by a coronagraph. For the measurements as presented here we have used a $3 \lambda/D$ Lyot coronagraph on a substrate.

To setup a high contrast measurement with well defined contrast ratios between planets and star we first setup an intensity measurement as shown on the top left of Figure 10 with relatively high intensities. This is a measurement without coronagraph. The intensity of the star is such that it will saturate the detector. Therefore the star intensity is attenuated with an ND filter (a ND3 for this case). We measure the peak intensity (top left) and the polarization (bottom left) of all planets and the star. The star polarization is of order $1e-3$ and the typical planet polarization is about 0.2.

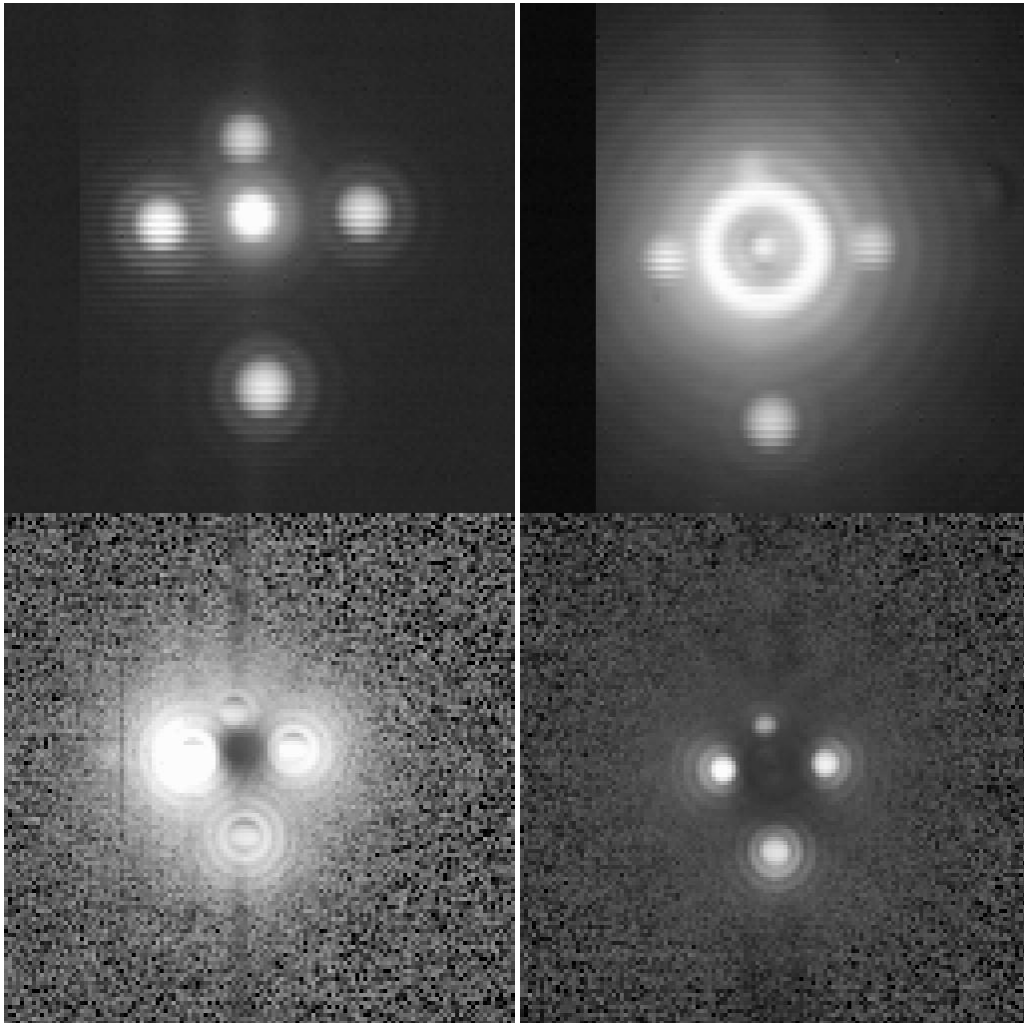


Figure 10. Illustrations of intensity (top) and polarization (bottom) images obtained with the ZIMPOL test bench without (left) and with (right) coronagraph. The planets in the focal plane represent the following angular separations from the star on the sky: top 70 mas, left 80 mas, bottom 150 mas and right 100 mas. Top Left: Intensity image with Star dimmed by ND3, Bottom Left: Polarization image of top left, Top Right: Coronagraphic intensity image of top left with ND3 removed, Bottom Right: Polarization image of top right

The images on the right (top is intensity and bottom is polarization) are just to show what happens when the coronagraph is inserted and the ND3 is removed from the star flux. The coronagraph halo, i.e. the intensity of the first bright ring is set such that it is just in the linear range of the detector.

For the high contrast measurements the intensity of the planets is reduced by ND filters. A typical result can be seen in Figure 11. The intensity contrast of the planet on the right is 10^{-6} and it is detected with a 25-sigma level. So in principle we could have detected a 5 times weaker signal still with a 5-sigma level. Therefore we conclude that we can reach a 5-sigma contrast of $(10^{-6})/5 = 2 \times 10^{-7}$ at 80 mas. Clearly we do not reach the expected overall 10^{-8} level yet.

It seems that we are mainly limited by the central star, i.e. diffraction rings that show up in polarization as a spatially modulated pattern around the PSF core and thereby it becomes the major noise source.

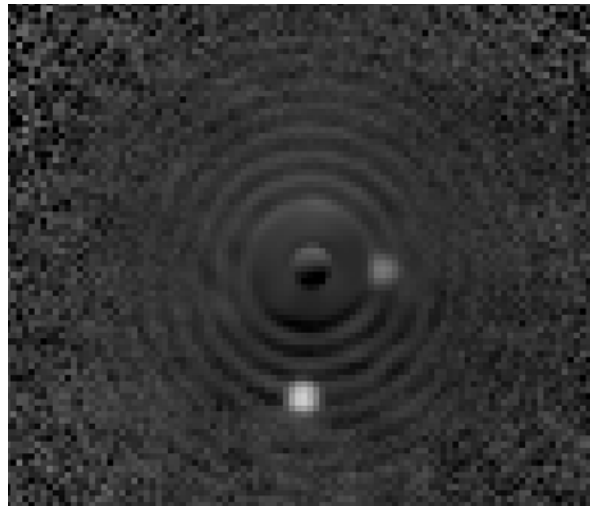


Figure 11 Double Difference high contrast image of very weak planets imaged very close to a very bright star. The planet at the right is at 80 mas from the star. The ring pattern that dominates the background noise can be clearly seen.

In the design phase we have anticipated a differential tilt effect of the FLC that shows up as a differential shift in the image plane. The HWP2 double difference technique was intended to calibrate this effect, i.e. by subtracting images taken with HPW2 at a zero position and a 45 degree rotated position the FLC effects should be removed. However, test images as shown in Figure 12 show polarized residuals of the coronagraph diffraction rings that do not subtract in single difference and also not in double difference.

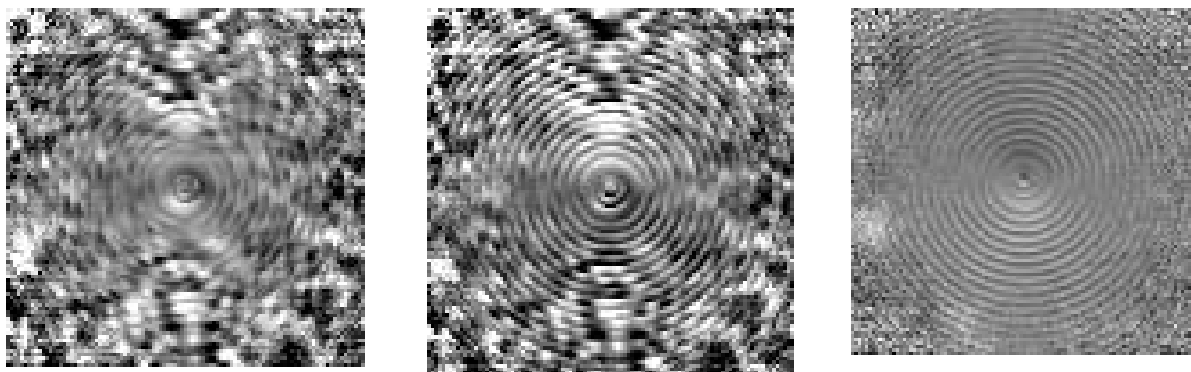


Figure 12. High contrast images to show the effect of differential beam shifts. (Left) Single Difference image with HWP2 at 0 deg (Middle) Single Difference image with HPW2 at 45 deg (Right) Double Difference image, i.e. subtraction of the two Single Difference images. Clearly the residual ring pattern is not removed in the Double Difference.

We have further looked into the issue and we see that the ring pattern is caused by differential shifts that are already present in the four sub frames that our used to calculate a single polarization image. There seem to be three contributions to differential shifts:

1. Detector offsets
2. FLC differential tilt
3. HWP2 birefringence or fiber effects (still under investigation)

Currently we can quantify the individual contributions but we don't have a complete understanding of the effects yet. Therefore activities in the next few months will be focused on a better understanding of the observed differential beam shifts and on strategies to correct for the differential shifts in the software before combining the sub images in order to improve the contrast.

3. CONCLUSIONS AND OUTLOOK

Intensive sub-system testing shows that ZIMPOL complies with all the major requirements. However, the point source sensitivity is currently limited by differential beam shifts that are not completely understood yet. Activities for the next few months will be focused on a better understanding and eventual compensation of the differential beam shift effects. ZIMPOL will be shipped to LAOG in Q4 2011 for integration with the SPHERE system. Overall system testing is foreseen for the first half year of 2012.

REFERENCES

- [1] Schmid, H. M., Beuzit, J.-L., Feldt, M., Gisler, D., Gratton, R., Henning, T., Joos, F., Kasper, M., Lenzen, R., Mouillet, D., Moutou, C., Quirrenbach, A., Stam, D. M., Thalmann, C., Tinbergen, J., Verinaud, C., Waters, R., and Wolstencroft, R., "Search and investigation of extra-solar planets with polarimetry," IAU Colloq. 200, 165–170 (2006)
- [2] D. Gisler, H.M. Schmid, C. Thalmann, H.P. Povel, J.O. Stenflo, F. Joos, M. Feldt, R. Lenzen, J. Tinbergen, R. Gratton, R. Stuik, D.M. Stam, W. Brandner, S. Hippler, M. Turatto, R. Neuhäuser, C. Dominik, A. Hatzes, Th. Henning, J. Lima, A. Quirrenbach, L.B.F.M. Waters, G. Wuchterl, H. Zinnecker, CHEOPS/ZIMPOL: a VLT instrument study for the polarimetric search of scattered light from extrasolar planets. in: "Ground-based instrumentation for astronomy", A.F.M. Moorwood & M. Iye (eds.), SPIE Conf. Vol. 5492, 463-474 2004
- [3] Beuzit, J.-L., Feldt, M., Dohlen, K., Mouillet, D., Puget, P., Antichi, J., Baruffolo, A., Baudoz, P., Berton, A., Boccaletti, A., Carbillet, M., Charton, J., Claudi, R., Downing, M., Feautrier, P., Fedrigo, E., Fusco, T., Gratton, R., Hubin, N., Kasper, M., Langlois, M., Moutou, C., Mugnier, L., Pragt, J., Rabou, P., Saisse, M., Schmid, H. M., Stadler, E., Turrato, M., Udry, S., Waters, R., and Wildi, F., "SPHERE: A 'Planet Finder' Instrument for the VLT," The Messenger 125, 29–34 (2006)
- [4] Roelfsema, R., Schmid, H.M., Pragt, J., Gisler, D., Waters, R., Bazzon, A., et al, "The ZIMPOL high-contrast imaging polarimeter for SPHERE: design, manufacturing, and testing," Proc. SPIE 7735, 77354B-77354B-17 (2010)
- [5] D. M. Stam, Spectropolarimetric signatures of Earth-like extrasolar planets, A&A 482, 989-1007 (2008)
- [6] E. Buenzli, H.M. Schmid: A grid of polarization models for Rayleigh scattering planetary atmospheres, Astron. Astrophys. 504, 259-276, 2009
- [7] Wildi, F., et al, The performance of SPHERE in the integration lab, Proc. SPIE, Paper 8151-22 (2011)